Atmospheric Environment 368 (2026) 121761

Contents lists available at ScienceDirect

Atmospheric Environment

journal homepage: www.elsevier.com/locate/atmosenv

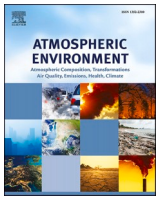

Source apportionment of carbonaceous submicron particulate matter in an urban area synthesizing the results of observation- and chemical transport model-based approaches

Evangelia Siouti [a], Ksakousti Skyllakou [a], David Patoulias [a], Eleni Athanasopoulou [c], Jeroen Kuenen [d], Marta Via [g], Marjan Savadkoohi [e,f], María Cruz Minguillón [e], Marco Pandolfi [e], Andrés Alastuey [e], Xavier Querol [e], Spyros N. Pandis [a,b,*]

[a] Institute of Chemical Engineering Sciences (ICE-HT), Foundation for Research and Technology Hellas (FORTH), Patras, 26504, Greece
[b] Department of Chemical Engineering, University of Patras, Patras, 26504, Greece
[c] Institute for Environmental Research and Sustainable Development, National Observatory of Athens (NOA), Athens, 11810, Greece
[d] TNO, Department of Climate, Air and Sustainability3584 CB Utrecht, the Netherlands
[e] Institute of Environmental Assessment and Water Research (IDAEA-CSIC), 08034, Barcelona, Spain
[f] Department of Natural Resources & Environment, Industrial & TIC Engineering (EMIT-UPC), Manresa, Spain
[g] University of Nova Gorica, Centre for Atmospheric Research (CRA), Ajdovščina 5270, Slovenia

HIGHLIGHTS

- Combination of observation and CTM-based source apportionments for PM_1.
- Ability to apportion secondary PM and PM from long-range transport.
- Oxygenated OA is the major OA component even in an urban area.
- Improvements needed for the simulation of secondary OA in winter.
- Emissions of EC from biomass burning are overpredicted.

ABSTRACT

Particulate matter (PM) significantly impacts urban air quality and public health, making the quantification of its source contributions crucial for effective air quality management. In this work, we investigate the origins of organic aerosol (OA) and elemental carbon (EC) in an urban environment by synthesizing results from *in situ* observational analyses (receptor modeling) and chemical transport modeling. This study focused on the city of Barcelona, Spain, during a summer and a winter period in 2019, using measurement data from an aerosol chemical speciation monitor (ACSM), an Aethalometer, and analyses of filter samples along with source-resolved predictions from the chemical transport model (CTM) PMCAMx. Results refer to PM_1 (PM finer than 1 μm). Oxygenated OA (OOA) was the dominant source of OA during both periods with contributions ranging from 63 % of PM_1 OA in winter to 80 % in summer. During summer, most of it originated from sources outside Barcelona such as wildfires, biogenic sources, as well as sources outside Europe. PMCAMx significantly underpredicted OOA during wintertime, suggesting that the model is lacking both processes that produce secondary OA (SOA) during periods of low photochemical activity and the corresponding emissions of organic pollutants. Biomass burning OA (BBOA) emitted far away from the city and its conversion to SOA either due to nighttime or aqueous chemistry could explain part of the missing OOA. Hydrocarbon-like OA (HOA) ranged from 8 to 14 % of the OA in both periods, peaking during morning and evening rush hours. The primary OA (POA) emissions from transportation during winter may be underestimated in the emission inventory. Cooking OA (COA) was also a significant source (11 % of total PM_1 OA) and it needs to be added to the current European emission inventories. Fresh BBOA was a small component of OA during summer and higher during winter. The PM_1 EC levels were found to be dominated by local sources during both seasons. Among these sources, fossil fuel combustion was the most important contributor, accounting for approximately 74 % of the total EC. This highlights the strong influence of traffic and other fossil fuel-related activities on EC concentrations in Barcelona, regardless of season.

This study demonstrates the value of integrating observational data (and receptor modelling) with chemical transport modeling to more accurately identify the sources of carbonaceous PM in urban environments. Such combined approaches are essential for developing effective mitigation strategies tailored to seasonal and local emission patterns, ultimately supporting improved air quality management.

* Corresponding author. Institute of Chemical Engineering Sciences (ICE-HT), Foundation for Research and Technology Hellas (FORTH), Patras 26504, Greece
E-mail address: spyros@chemeng.upatras.gr (S.N. Pandis).

https://doi.org/10.1016/j.atmosenv.2025.121761
Received 20 October 2025; Received in revised form 13 December 2025; Accepted 28 December 2025
Available online 31 December 2025

1. Introduction

PM has significant impacts on air quality, human health, climate change, and visibility (IPCC, 2021; WHO, 2024). Fine particles (those finer than 1 or 2.5 μm, PM_1 and $PM_{2.5}$) are especially harmful as they can penetrate deep into the respiratory system, contributing to numerous health issues. Exposure to high $PM_{2.5}$ concentrations has been associated with increased respiratory and cardiovascular morbidity and premature mortality, but also with neurodegenerative issues and cancer (WHO, 2024). At the same time, PM influences the Earth's radiative balance by absorbing and scattering sunlight and by acting as cloud condensation nuclei (Seinfeld and Pandis, 2016).

Carbonaceous PM includes organic and elemental carbon (OC and EC, respectively). These particles enter the atmosphere either through direct emission, primarily from incomplete combustion of fossil fuels, biomass burning and biogenic activity, or through secondary formation during the oxidation of organic vapors. OA often constitutes a significant, and in some cases dominant, fraction of submicron PM across diverse environments (Jimenez et al., 2009). EC is chemically inert and emitted into the atmosphere as a primary pollutant. EC absorbs light contributing significantly to atmospheric warming (Bond and Bergstrom, 2006; IPCC, 2021).

Given the complexity and environmental significance of carbonaceous PM, advanced instrumentation and receptor modeling (RM) tools have become essential for characterizing its composition and sources. In recent years, the Aerosol Mass Spectrometer (AMS) has been widely used in field studies, offering detailed insights into the chemical composition of atmospheric aerosols (DeCarlo et al., 2008; Drewnick et al., 2005; Jayne et al., 2000; Jimenez et al., 2009). A decade later, Ng et al. (2011) developed the Aerosol Chemical Speciation Monitor (ACSM), which is based on AMS technology but designed for more cost-effective long-term monitoring of non-refractory submicron aerosol composition. The ACSM has been used in conjunction with RMs (mainly Positive Matrix Factorization, PMF) to determine the sources of OA (Chen et al., 2022; Petit et al., 2014; Zografou et al., 2022).

The Aethalometer absorption measurements at seven wavelengths can be used to apportion black carbon (BC) to liquid and solid fuel combustion (Liu et al., 2018, 2021; Sandradewi et al., 2008). The term equivalent BC (eBC) is used when the mass concentration of BC is obtained from filter absorption photometers including the aethalometer. The measurement of eBC is based on a conversion factor (the Mass Absorption Cross Section, MAC) used to convert the measured absorption (at 880 nm from Aethalometers) to BC mass concentration (Petzold et al., 2013).

Other EC and OC source apportionment methods include ^{14}C radiocarbon analysis, the PMF model that utilizes trace elements to identify sources, Chemical Mass Balance (CMC), the macro-tracer method and various specialized RMs (Briggs and Long, 2016; Kumar et al., 2024; Zotter et al., 2014).

Chemical transport models are often used in combination with various methods to trace the origins of particulate matter. One of the most straightforward methods is known as the "zero-out" or "brute-force" approach (Koo et al., 2009; Park et al., 2003). This method involves running the CTM several times, each time eliminating emissions from a specific source category. Although effective, it is computationally demanding due to the need for multiple model simulations, one for each targeted source. Other methods used include the decoupled direct method (DDM), which computes the first-order sensitivity of pollutant concentrations to perturbations in input parameters, representing the linear response of the system, and the source-oriented external mixture (SOEM), which extends the DDM approach by computing second-order sensitivities. Developed by Wagstrom et al. (2008), the Particle Source Apportionment Technology (PSAT) algorithm is used in combination with CTMs to estimate the source contributions to PM components (Koo et al., 2009; Siouti et al., 2025; Skyllakou et al., 2017).

The main advantage of the RMs is that they do not depend on emission estimates, and they usually do not require detailed meteorological fields and process descriptions. On the other hand, they have limitations, such as their low spatial representativeness, and their inability usually to quantify the sources of secondary inorganic and organic aerosols. CTMs have several advantages, such as high spatial coverage and the ability to predict effects of specific air quality policy actions accounting for non-linear processes. However, they also have major limitations starting with the accuracy and completeness of the emission inventories, and the uncertainties in the simulation of atmospheric chemical and physical processes. Our hypothesis in this work is that combining RMs and CTMs can result in improved source apportionment.

There are several studies focusing on the urban area of Barcelona (NE Spain), investigating OA and eBC sources using RM-based source apportionment techniques. Mohr et al. (2012) reported that COA was the dominant primary component contributing 17 % to total OA at an urban background site in Barcelona during March 2009. HOA accounted for 16 % of total OA, while BBOA associated with heating and agricultural waste burning contributed 11 %. The remaining 55 % of total OA was attributed to SOA. Via et al. (2021) investigated the sources of PM_1 at the same urban background site in Barcelona, Palau Reial, during two periods: May 2014–May 2015 and September 2017–October 2018. They found that OOA (largely attributed to SOA) accounted for 57–70 % of PM_1 OA, HOA contributed 12–19 %, COA 14–18 %, and BBOA 4–6 %. Similar findings for August–September 2013 were reported from Minguillón et al. (2016), where COA was the dominant primary component (17 %) of total OA, while SOA contributed 73 %, and HOA the remaining 10 %. For eBC, a source apportionment analysis conducted in the same site using an aethalometer model indicated that 84 % of eBC was due to traffic and 16 % due to residential and commercial biomass combustion sources (Savadkoohi et al., 2023).

Modeling studies predicting air quality in Barcelona using CTMs are limited, and none has specifically examined the sources of the OA and EC in the area. Soret et al. (2014) utilized the CMAQ model at high-spatial resolution (1×1 km^2) over Barcelona and Madrid to assess potential air quality improvements resulting from different fleet electrification scenarios. Benavides et al. (2019) applied the CALIOPE-Urban v0.1 system, which is based on CMAQ, to estimate the NO_2 concentrations in Barcelona, but source apportionment was not included in their work.

The integration of results from RM and CTM to better understand the sources of OA and EC in urban areas has received little attention. In this study, we conducted a more detailed analysis focused on Barcelona, selected as a pilot city due to the availability of comprehensive measurements. Results from RMs and CTM were combined to provide detailed insights into the sources of OA and EC, and to identify potential contributors to discrepancies between CTM predictions and observational data. We applied the PMCAMx CTM with the source-apportionment PSAT algorithm, along with the method developed in Siouti et al. (2025) for the source apportionment of aerosol transported from outside the simulated urban area, in combination with advanced instrumentation, to estimate both local and transported sources of the major PM components in the city of Barcelona during a summer and winter month.

2. PMCAMx description and application

2.1. Model description

This study uses the three-dimensional chemical transport model PMCAMx (Particulate Matter Comprehensive Air quality Model with extensions) (Fountoukis et al., 2011; Tsimpidi et al., 2010) to simulate the air pollution levels in Barcelona, Spain. At each simulation step, the process begins with the addition of emissions from all contributing sources. This is followed by simulation of vertical and horizontal advection, chemical transformations, dispersion in all directions, and

removal through dry and wet deposition. To model the changes in aerosol mass size distribution and composition, a 10-bin sectional aerosol approach (size range from 30 nm to 40 μm) is employed, based on the method of Gaydos et al. (2003), assuming that all particles in each size bin have the same composition. An extended SAPRC mechanism (Carter, 2000) was used for gas-phase chemistry, which involves 217 reactions and 114 species (including 16 radicals and 76 gases). For aerosol chemistry, the bulk equilibrium approach was applied to partition inorganic and secondary organic compounds between the gas and particle phases (Capaldo et al., 2000). Aqueous-phase chemistry was simulated using the Variable Size Resolution Model of Fahey and Pandis (2001). Dry deposition was simulated using the methodology of Wesely (2007) and Slinn and Slinn (1980), whereas for wet deposition a scavenging model for aerosol and gases was applied (Seinfeld and Pandis, 2016). The approach of Tambour and Seinfeld (1980) was employed to model aerosol particle coagulation. Organic aerosol evolution was modeled using the Volatility Basis Set (VBS) approach. The 1-D VBS method (Donahue et al., 2006) was used for both primary and secondary OA, considering them semi-volatile and chemically reactive. The organic components were simulated using 8 volatility bins ranging from saturation concentration of 10^{-1} to 10^{6} μg m^{-3} at 298 K. The parameterization used follows the work of Tsimpidi et al. (2010).

2.2. Model application

In this study a summer (July 1–31) and a winter period (January 18 to February 28) during 2019 were simulated. PMCAMx was applied over Europe with a 36 × 36 km^2 spatial resolution focusing on the urban area of Barcelona using three nested grids with increasing spatial resolution (12x12, 3x3 and 1 × 1 km^2). The outer European domain, which had the lower spatial resolution (36 × 36 km^2), extended over an area of 5400 × 5832 km^2 (Fig. 1). The inner domain, which is the high-resolution domain, covers a region of 72 × 72 km^2 for the city using 1 × 1 km^2 spatial resolution. The other two intermediate grids of 12x12 and 3 × 3 km^2 resolution were centered on the city. In the vertical, 14 layers were used for each of the modeling domains. A rotated polar stereographic map projection was used.

The Weather Research and Forecasting (WRF) mesoscale numerical prediction model (Skamarock et al., 2019) was applied to produce meteorological data for these periods by using the same gridded domains as PMCAMx. WRF output was used for both the 36 × 36 km^2 European domain and the innermost 1 × 1 km^2 domain. For the intermediate nested domains with resolutions of 12 × 12 km^2 and 3 × 3 km^2, meteorological data were generated through interpolation based on a zooming approach. Additional information can be found in Siouti et al. (2022, 2024).

2.2.1. Emissions

Anthropogenic emissions were obtained from the CAMS-REG-v4 inventory, developed by the Netherlands Organization for Applied Scientific Research (TNO), with a spatial resolution of 0.05° × 0.1° characterized as “area” and “point” sources (Kuenen et al., 2022). This inventory organized emissions into twelve categories, including industrial processes, electricity generation, road and off-road transport, shipping and aviation, residential activities, fugitive and solvent sources, waste burning, agriculture, and agricultural burning. It accounts for key air pollutants such as SO_2, NO_x, volatile organic compounds (VOCs), NH_3, CO, PM_{10} (PM finer than 10 μm), and $PM_{2.5}$. Intermediate volatility organic compounds (IVOCs) are included in the emissions and are assumed to be equal to 1.5 times the primary organic aerosol emissions (Tsimpidi et al., 2010) Emissions from major “point” sources like industry, heating plants, airports, and waste processes were allocated to their respective grid cells. Additional details are available in Siouti et al. (2025).

To produce high-resolution emission data for the inner domain, the original TNO inventory was downscaled using the UrbEm method and tool (Ramacher et al., 2021). UrbEm combines the CAMS emissions data with carefully selected high-resolution spatial proxies that correspond to each emission sector. This tool enables the creation of emission inventories for any European region or city at a specified resolution. In this study, the UrbEm output was normalized and used to redistribute the TNO emissions onto a 1 × 1 km^2 grid, preserving the total emission quantities. The daily emissions for the high-resolution domain are summarized in Table 1 for the two periods.

Biogenic and marine emissions are also accounted for in the model. The MEGAN v3 algorithm (Guenther et al., 2012; 2020) is applied to generate hourly, gridded biogenic emissions for both the European and urban domain. It estimates emissions for 201 individual gas-phase compounds, which are subsequently grouped into 27 modeled species, including isoprene, monoterpenes, and sesquiterpenes. For marine aerosol sources, the model incorporates size-resolved sea-salt and marine organic particles. The O'Dowd distribution (O'Dowd et al., 2008) is

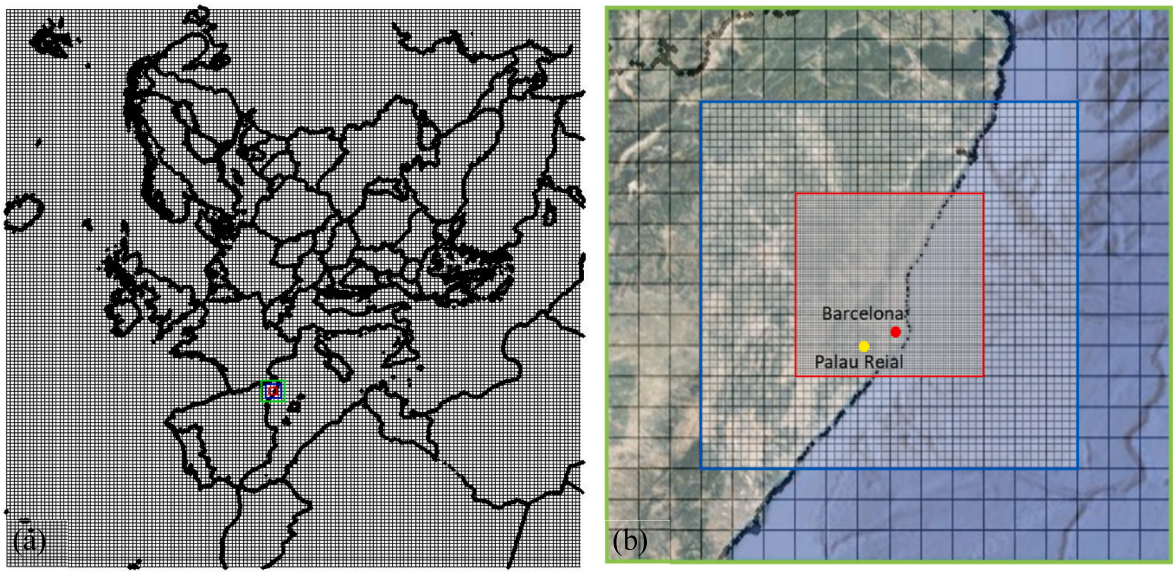

Fig. 1. (a) The European domain with the low-spatial resolution of 36 × 36 km^2 and (b) the nested domains focusing on the high-resolution urban area of Barcelona. The study site of Palau Reial is also shown.

used for sea-salt and organic aerosols with diameters up to 1 μm, while the Monahan distribution (Monahan et al., 1986) is applied for larger, super-micrometer sea-salt particles.

2.3. Model evaluation

The mean bias (MB), fractional bias (FBIAS), mean error (ME) and fractional error (FERROR) were used for the evaluation of model performance of OA, EC and their sources. The evaluation metrics are given by the following equations:

$$MB = \frac{1}{N}\sum_{i=1}^{n}(P_i - O_i) \quad ME = \frac{1}{N}\sum_{i=1}^{n}|P_i - O_i|$$

$$FBIAS = \frac{2}{N}\sum_{i=1}^{n}\frac{(P_i - O_i)}{(P_i + O_i)} \quad FERROR = \frac{2}{N}\sum_{i=1}^{n}\frac{|P_i - O_i|}{(P_i + O_i)} \tag{1}$$

where N is the total number of measurements, P_i is the predicted concentration and O_i is the corresponding measured concentration of the evaluated species.

Based on Morris et al. (2005) PM model performance for hourly average values is considered excellent for FBIAS $\leq \pm 15$ % and FERROR $\leq \pm 35$ %, good for FBIAS $\leq \pm 30$ % and FERROR $\leq \pm 50$ %, average for FBIAS$\leq \pm 60$ % and FERROR $\leq \pm 75$ %, while there are fundamental problems in the modeling system for higher FBIAS and FERROR.

3. Measurements

PM_1 non-refractory components were measured using an ACSM with a Quadrupole spectrometer (Q-ACSM, Aerodyne Research Inc.), operating at a time resolution of 30 min and unit mass spectral resolution. For this study, the periods, subject to instrument measurements availability, ranged from January 18–28 and February 3–28 for winter, and July 1–31 to represent summer. The measurements were carried out in Palau Reial, (41° 23′01500″ N, 02° 07′00500″ E; 80 m a.s.l.), an urban background site in the NW of Barcelona. The site is located 200 m away a major road (Avenue Diagonal) and near a residential area. The Q-ACSM was connected to a 2.5 μm cutoff with a flow rate of 3 L min^{-1} sampling through a Nafion drier maintaining RH<40 %. The ACSM had an internal sample flow rate of 0.08 L min^{-1}. Concentrations of OA, sulfate, nitrate, ammonium, and chloride were estimated using the fragmentation table of Allan et al. (2004) and ammonium nitrate and ammonium sulfate calibration values (RF = 5.1 10^{-11}, RIE_{NH4} = 4.35, RIE_{SO4} = 0.67). Collection efficiency (Middlebrook et al., 2012), air beam, and ion transmission corrections were applied. Data acquisition and treatment software versions 1.6.0.0 and 1.6.1.1 were implemented in Igor Pro (Wavemetrics, Inc.). An intercomparison of the total NR-PM_1 and the sum of the concentrations of its individual components measured with co-located independent instrumentation was conducted to ensure the quality of the measurements (COST-COLOSSAL, 2019).

OA source apportionment was conducted using the multilinear engine (ME-2) (Paatero, 1999). The OA matrices were limited to 12–120 Th in the spectral range. The Source Finder software (SoFi, Datalystica Ltd., Canonaco et al., 2021) and the protocol established by Chen et al. (2022) were used to determine OA sources. Profile anchors extracted from winter unconstrained solutions were used as a priori knowledge in ME-2. The final ME-2 solution identified five OA sources in winter: HOA, COA, BBOA, less oxidized oxygenated OA (LO-OOA), and more oxidized oxygenated OA (MO-OOA) and four sources in summer, excluding BBOA.

In this study, the filter absorption photometer used was the Aethalometer (model AE33, Magee Scientific). The Aethalometer was chosen because it enables the estimation of fossil fuel and biomass burning combustion sources applying the aethalometer source apportionment approach (Sandradewi et al., 2008). The AE33 measures light attenuation across seven wavelengths (370, 470, 520, 590, 660, 880, and 950 nm) on an aerosol-loaded filter tape. The AE33 converts optical absorption coefficients to eBC mass concentrations using a nominal MAC of 7.77 m^2 g^{-1} at 880 nm. Filter loading effect is corrected in real time through built-in dual-spot algorithm (Drinovec et al., 2015). eBC values were corrected using the methodology described in Savadkoohi et al. (2023, 2024) to ensure accurate mass concentration estimates.

Furthermore, daily PM_1 samples were collected in the study period in one out four days collected by a high volume MCV sampler (30 m^3 h^{-1}) for PM_1 chemical speciation analyses (Querol et al., 2001). Moreover, OC and EC analyses were carried out using a Sunset thermo-optical analyzer and the EUSSAR-2 protocol (Cavalli et al., 2010).

Table 1
Daily PM_1 emissions (tn) for the high-resolution domain during the summer and winter periods.

Emissions (tn d^{-1})	Summer	Winter
EC (total)	2	6.4
EC (biomass burning)	0.65	5
EC (fossil fuel)	1.3	1.2
EC other	0.15	0.2
OA (total in VBS)	5	14
OA (biomass burning)	1.35	10.4
Sulfate	0.12	0.14
Crustal	3.3	4.4
Sodium	0.2	0.5
Chloride	0.32	0.75

4. Results

4.1. Summertime OA and its sources

During the summer period, total PM_1 OA had an average measured concentration of 2.7 μg m^{-3} equal to the predicted value. The average diurnal profile of measured total PM_1 OA and its predicted sources in summer are shown in Fig. 2a. According to the measurements, OA peaked from 9:00 to 11:00 LT, due to increasing OOA levels (Fig. S1). During this period, the model underpredicted OA, likely due to a missing or underestimated source or process.

Sources outside the Barcelona area dominated the total PM_1 OA, contributing 85 % of the total, according to the PMCAMx predictions (Fig. 3a). 25 % of the transported OA originated from wildfires, 23 % from sources outside Europe, 22 % from biogenic and marine sources, 11.6 % from industry and fugitives and solvents, 8 % from agriculture and waste burning and 5.3 % from combustion. Smaller contributions came from road transport (2 %), shipping (1.7 %), non-road transportation (1.2 %), and aviation (0.2 %). Local sources had lower contributions, with 3.8 % of the total PM_1 OA from road transport, 3.3 % from agriculture and waste burning, 2.6 % from industry and fugitives and solvents, 1.7 % from shipping and 1.7 % from biogenic and marine sources. Contributions from combustion, off-road traffic, and aviation were all below 1 %.

4.1.1. Evaluation including comparison with PMF results

OOA accounted for 80 % of the total PM_1 OA during the summer, based on ACSM measurements. The average measured OOA concentration was 2.2 μg m^{-3}, while the corresponding predicted CTM's concentration was approximately 2.5 μg m^{-3}. Fractional bias (<35 %) and fractional error (<50 %) also indicated a good model performance for this source (Table 2). Throughout the day, both measured and predicted OOA showed a similar diurnal pattern, reflecting that most OOA originates from transport outside Barcelona rather than local sources (Fig. 4). A peak was observed in the measurements during the morning hours (9:00–11:00 LT), which may be related to entrainment from upper atmospheric layers or local production.

Sources outside Barcelona were the dominant source of OOA during summer (92 %) based on PMCAMx. Transported OOA was primarily

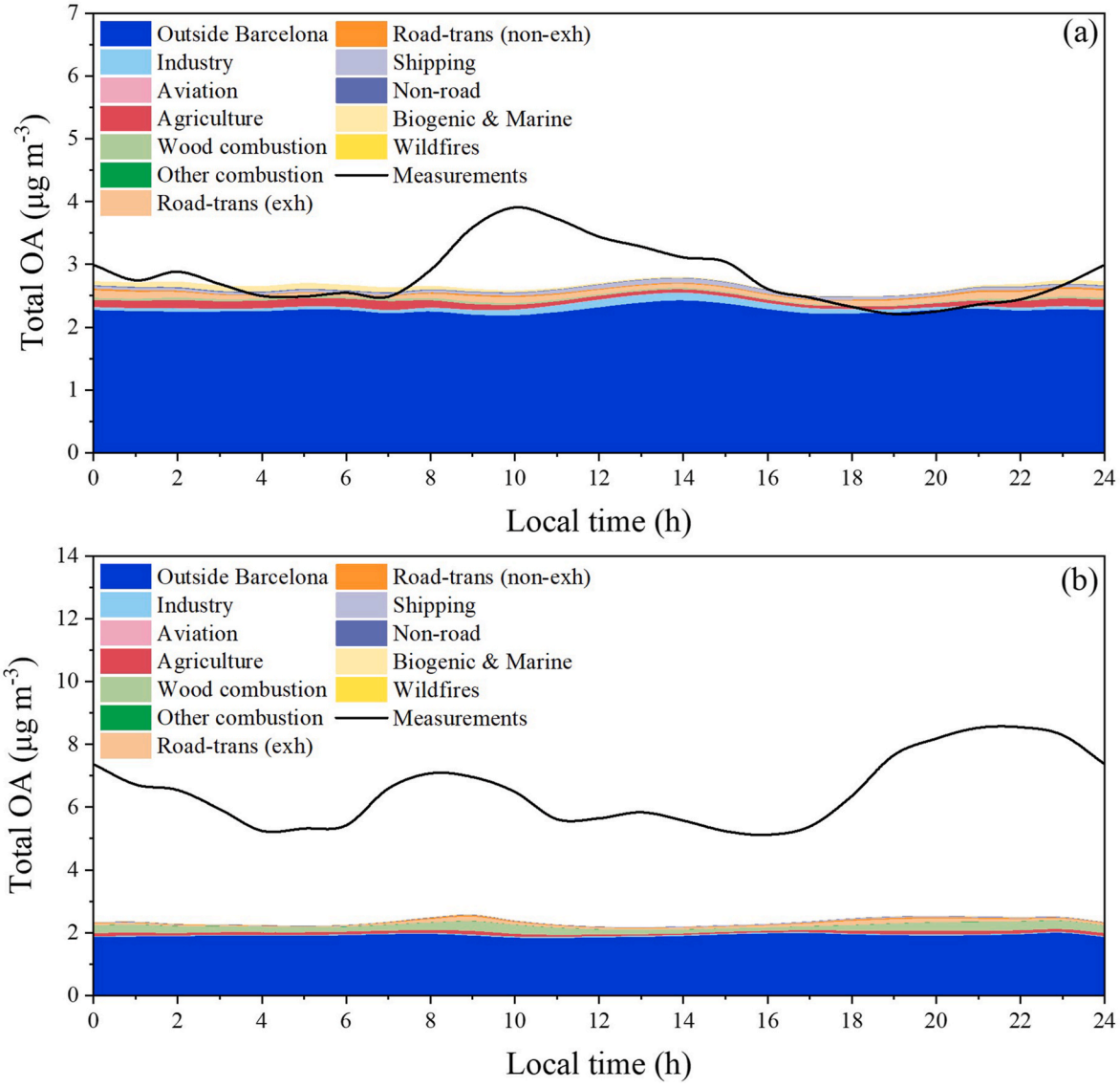

Fig. 2. Average diurnal profiles of measured and predicted OA during (a) summer and (b) winter period in Palau Reial. The predicted sources of OA are also shown.

attributed to wildfires (22 %), sources outside Europe (21 %), marine and biogenic sources (19 %), industry and fugitives and solvents (10.4 %) and agriculture and waste burning (8.5 %). Additional contributions included domestic combustion (4 %), road transport (4 %), shipping (2 %), non-road transportation (1 %), and aviation (0.1 %).

HOA was measured to contribute 9 % to the total PM_1 OA with an average concentration of 0.25 μg m^{-3} (Table 2). Measurements had a peak at 9:00 LT probably due to local transportation, which was underpredicted by the model. This finding indicates the potential underestimation of local transportation sources during this morning period (Fig. 4).

The dominant HOA sources were predicted to be local agricultural and waste burning processes (36 % of HOA), local road transportation (29 %), sources outside Barcelona (16 %), shipping (10 %), industry (5 %), and non-road transportation (3 %). 98 % of the sources outside Barcelona were due to marine and biogenic sources, and the remaining due to aviation.

Fresh BBOA was not detected by the ACSM measurements during this period. This finding was consistent with PMCAMx that predicted that total BBOA was below 1 % of total OA (0.02 μg m^{-3}).

Cooking OA contributed 11 % to total PM_1 OA in summer, with an average concentration of 0.3 μg m^{-3} according to the ACSM analyses, while the current emission inventory is missing that source. Measured COA peaked during the morning, lunch and dinner hours (Fig. S1). Hourly concentrations of the contributions of OA sources as well as their mass spectra are presented in Figs. S2 and S3.

4.2. *Summertime EC and its sources*

The average PM_1 EC concentration was 0.64 μg m^{-3} for predictions and 0.7 μg m^{-3} for eBC measurements. During the day, the EC peaked during the morning, at 9:00 LT, up to 1.2 μg m^{-3} and it began to rise again after 20:00 LT (Fig. 5a). During the rest of the day, average EC concentrations remained lower. Based on model predictions, peaks in concentration during the morning and night were due to road transport.

Most of the predicted EC was attributed by the CTM to local road transport (42 %) on average (Fig. 3a). Transported EC from other areas contributed 25 % to the total EC in summer, and local shipping accounted for 13 %. Other significant local sources included combustion and agricultural and waste burning processes, each contributing 8 % to the total EC. Transported EC was mainly due to combustion (44 %), sources outside Europe (40 %) and wildfires (15 %), with a lower contribution from industry and fugitives and solvents (2 %).

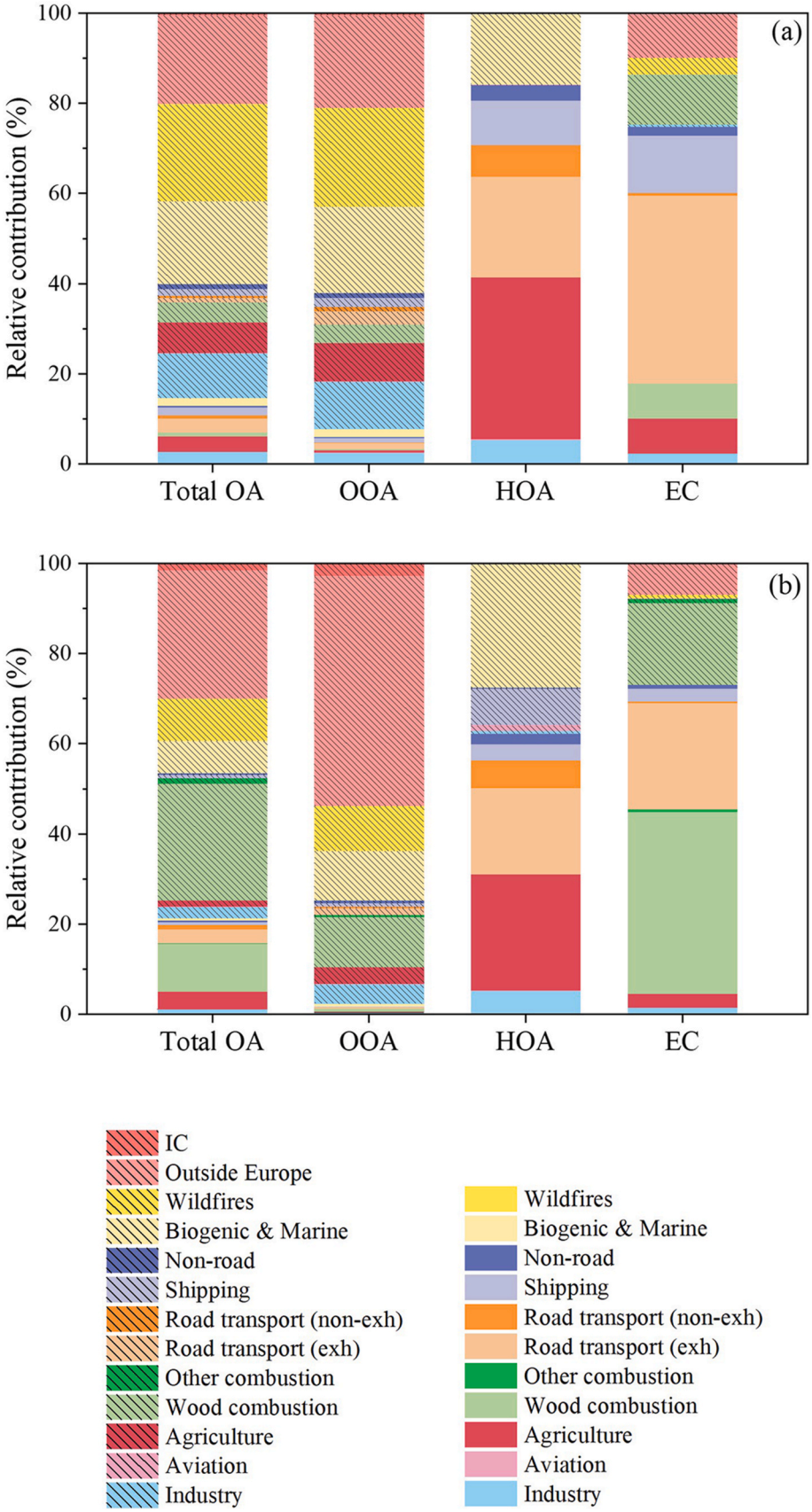

Fig. 3. Predicted source contributions of PM_1 components during (a) summer and (b) winter period in Palau Reial.

Table 2
Metrics for hourly averaged PM_1 OA components comparing PMCAMx predictions and measurements during the summer and winter periods at Palau Reial.

	Predicted (μg m^{-3})	Measured (μg m^{-3})	FBIAS (%)	FERROR (%)	MB (μg m^{-3})	ME (μg m^{-3})
Summer						
COA	–	0.3	–	–	–	–
HOA	0.21	0.25	−3	60	−0.04	0.15
OOA	2.46	2.2	12	42	0.21	0.95
BBOA	0.02	–	–	–	–	–
Winter						
COA	–	0.8	–	–	–	–
HOA	0.3	1	−46	> ±75	−0.6	0.7
OOA	1.8	4.4	−73	> ±75	−2.6	2.7
BBOA	0.2	0.8	> ±75	> ±75	−0.57	0.6

4.2.1. *Evaluation including comparison with aethalometer source apportionment*

Fossil fuel combustion, mainly from road traffic, was identified by RM as the dominant source of eBC in summer. Analysis of aethalometer data showed an average measured concentration of 0.52 μg m^{-3}, corresponding to a 74 % contribution. The diurnal profile exhibited a morning peak at 09:00 LT and another in the early evening (Fig. 6a). In contrast, PMCAMx underpredicted EC from this source, with an average concentration of 0.38 μg m^{-3}.

Biomass burning contributed 26 % of the total eBC, with an average measured concentration of 0.17 μg m^{-3}. The diurnal profile showed two peaks, one in the morning and another in the afternoon (Fig. 6b). In comparison, the CTM underpredicted EC from this source, estimating an average concentration of 0.05 μg m^{-3} -about three times lower than the value obtained from aethalometer measurements (RM). Hourly metrics are presented in Table 3.

4.3. *Wintertime OA and its sources*

During wintertime, the model seriously underpredicted total OA during the whole day (Fig. 2b). The average measured concentration of PM_1 OA was 7 μg m^{-3} and the predicted value was 2.3 μg m^{-3}. Measured peaks were mainly attributed to OOA (mostly SOA) (Fig. S1).

The predicted OA was mainly due to transport from outside Barcelona (79 %) (Fig. 3b). Most of this was related to sources outside Europe (28.5 %), wood combustion (26 %), wildfires (9.4 %), and marine and biogenic sources (7.2 %). From the local sources, 10.6 % was attributed

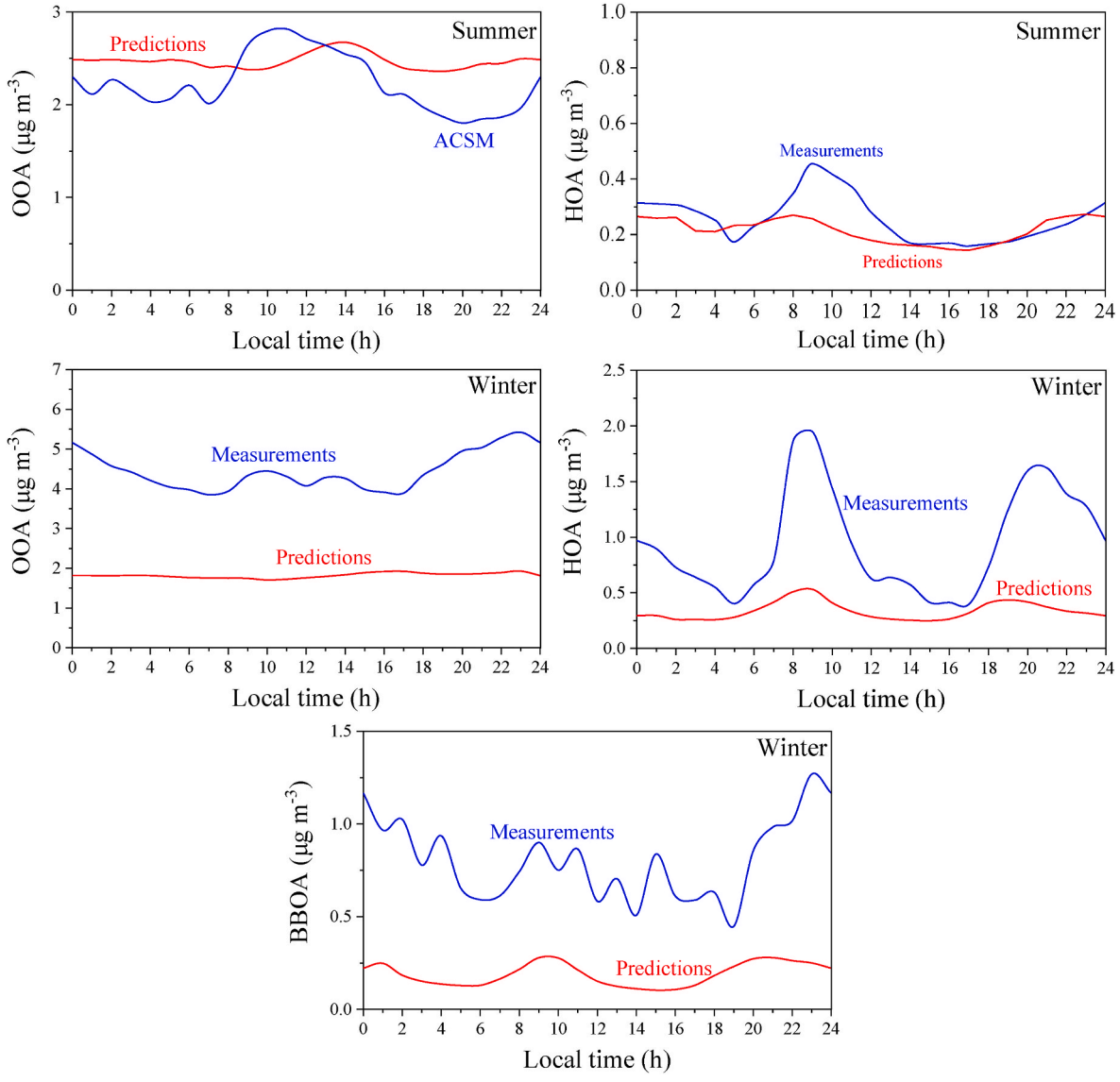

Fig. 4. Average diurnal profile of predicted and measured (a) OOA, (b) HOA in Palau Reial during the summer and winter period.

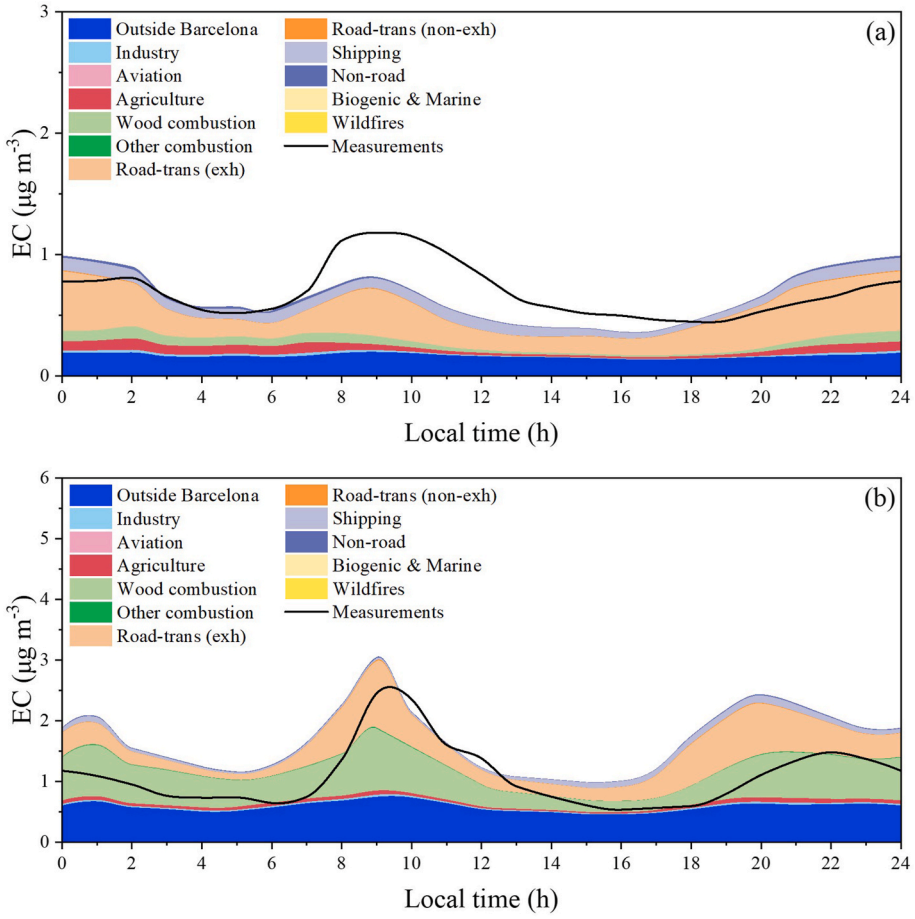

Fig. 5. Average diurnal profile of predicted EC and measured eBC in Palau Reial during the (a) summer and (b) winter period. Predicted local sources are also presented for both periods.

to wood combustion inside the city, 4 % to road transportation and 4 % to agriculture and waste burning processes.

4.3.1. Evaluation including comparison with PMF results

The ACSM suggested that 63 % of the total PM_1 OA was due to OOA during this period, with an average concentration of 4.4 μg m^{-3}, while the model predicted 1.8 μg m^{-3} (Table 2). The relatively flat average diurnal profiles indicated that a lot of it was probably due to transport from outside the Barcelona area (Fig. 4).

The model predicted that almost all OOA was due to transport from outside Barcelona (98 %) with most of it originating from outside Europe (51 %). The remaining was predicted to be due to domestic wood combustion (11.5 %), biogenic and marine sources (11 %), wildfires (10 %), industry and fugitives and solvents (4.3 %), agriculture and waste burning (3.7 %), initial conditions (2.8 %), road transport (1.8 %), shipping (0.9 %), domestic combustion from other fuels (0.5 %) and non-road transport (0.5 %). The rest comes from local sources.

HOA was identified as the second most important source of OA, contributing 14 % of the total PM_1 OA with an average concentration of 1 μg m^{-3}. However, the CTM underpredicted HOA concentrations by a factor of three (Fig. 4).

In winter, COA was measured at 0.8 μg m^{-3}, representing 11 % of the total PM_1 OA according to ACSM data. This source was missing from the current model application, highlighting its potential importance. COA concentrations peaked during the morning, lunch, and dinner hours (Fig. S1).

Fresh BBOA was detected by the ACSM only during the second part of the winter period, in February. PMCAMx predicted an average BBOA concentration of 0.2 μg m^{-3}, while the measured average during this time was 0.8 μg m^{-3}, accounting for 11 % of the total PM_1 OA. BBOA was consistently underpredicted throughout the entire period (Fig. 4).

4.3.2. Biomass burning

Fresh BBOA was detected only during the second winter period with an average concentration of 0.5 μg m^{-3}, whereas the predicted fresh BBOA was two times lower on average during the same period. However, fresh BBOA can age in the atmosphere both during the summer and the winter and may be detected as OOA by the ACSM.

Potassium (K) is often used as a tracer of biomass burning; however, it can also originate from other atmospheric sources, such as sea salt and mineral dust. Sea-salt K concentrations were calculated using the approaches of Lai et al. (2007) and Cao et al. (2016) relying on measured sodium (Na) concentrations ($K^+_{sea\text{-}salt} = 0.0355 \times Na^+_{sea\text{-}salt}$) and Fourtziou et al. (2017) baseed on magnesium (Mg) concentrations ($K^+_{sea\text{-}salt} = 0.3082 \times Mg^{2+}_{sea\text{-}salt}$). Both methods indicated that sea-salt K levels remained below 0.02 μg m^{-3} during all winter days (Table S2), suggesting that almost all the K came from sources other than sea salt. The contribution of dust to K concentrations was assessed by using measured calcium (Ca) concentrations. The dust-related K (K^+_{dust}) was calculated with equation $K^+_{dust}=0.2 \times Ca$ (Falkovich and Schkolnik, 2004; Ho et al., 2003; Kchik et al., 2015; Wang et al., 2006; Zhang et al., 2010). The calculated K^+_{dust} was found to be less than 0.04 μg m^{-3} on all winter days (Table S2). Since the sea-salt and the dust K^+ concentrations were quantified, the biomass burning potassium was calculated according to: $K^+_{bb}=K^+ - K^+_{sea\text{-}salt} - K^+_{dust}$. The $PM_{2.5}$ biomass burning K^+ concentration for each winter day is shown in Table S1, ranging from 0.02 to 0.14 μg m^{-3}.

The BBOA:K^+ ratio has been widely used in previous research to estimate BBOA concentrations and emissions, with reported values

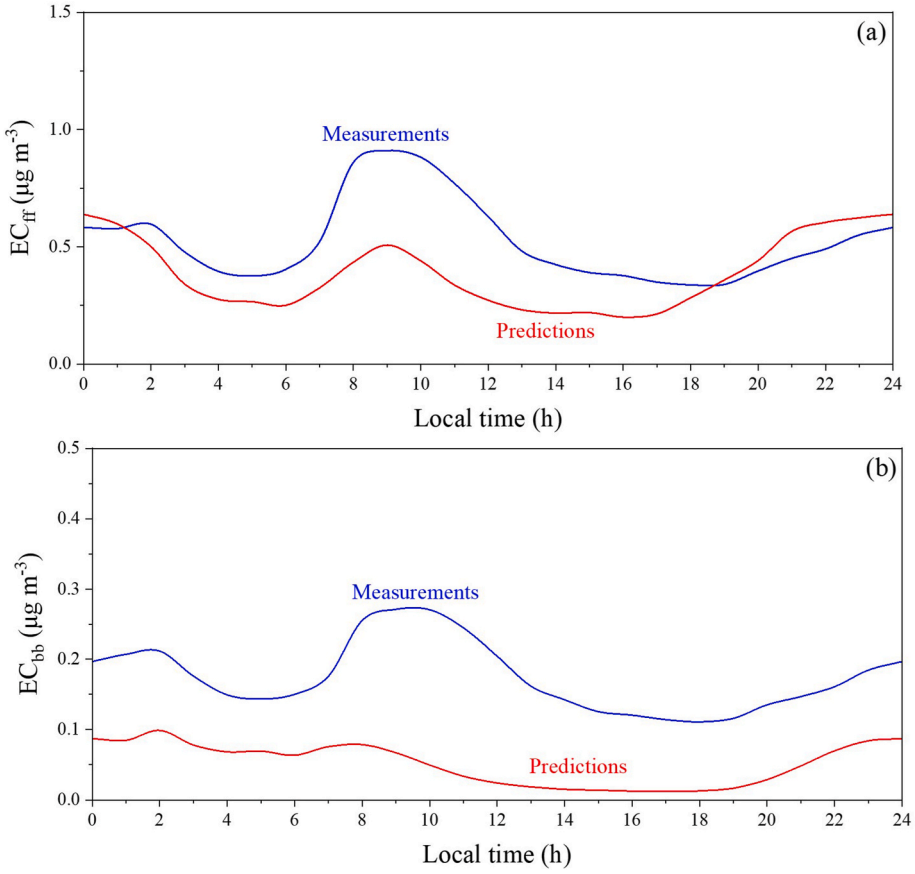

Fig. 6. Average diurnal profile of predicted EC and measured eBC from (a) fossil fuel and (b) biomass burning combustion in Palau Reial during the summer period.

Table 3
Metrics for hourly averaged PM_1 EC predicted and eBC measured concentrations of during the summer and winter periods.

	Average predicted (μg m^{-3})	Average measured (μg m^{-3})	FBIAS (%)	FERROR (%)	MB (μg m^{-3})	ME (μg m^{-3})
Summer						
EC_{ff}	0.38	0.52	−29	59	−0.14	0.29
EC_{bb}	0.05	0.17	>±75	>±75	−0.12	0.13
Winter						
EC_{ff}	0.52	0.8	−35	70	−0.27	0.5
EC_{bb}	0.53	0.3	43	73	0.23	0.3

ranging from 5 to 100, depending on combustion conditions and the degree of atmospheric aging (Zotter et al., 2014). In this study, we used an average BBOA:K^+ ratio of 20, as suggested by Seinfeld and Pandis (2016), to estimate wintertime BBOA concentrations. Using the mean daily $PM_{2.5}$ biomass burning K^+ concentrations, we calculated daily average BBOA levels ranging from 0.4 to 2.8 μg m^{-3} (Table 4). If we consider the full range of BBOA:K^+ ratios reported in the literature (5–100), the estimated average daily BBOA concentrations could vary between 0.1 and 14 μg m^{-3}. This analysis suggests that there could be significant amounts of aged BBOA present in the area during the winter and they could explain part of the OOA that is underpredicted by the model. Given the relatively low photochemical activity during this period nighttime oxidation of BBOA could be a key route for SOA formation (Kiendler-Scharr et al., 2016; Kodros et al., 2022; Tiitta et al., 2016).

4.4. *Wintertime EC and its sources*

The average CTM predicted PM_1 EC concentration was 1.7 μg m^{-3} and the average measured eBC was 1.1 μg m^{-3} for the period of available measurements. During the day, the predicted EC had a peak during the morning, at 9:00 LT and another one during the evening, at 20:00 LT due to road transport and domestic wood combustion (Fig. 5b). Measurements indicated similar behavior during the day, but the nighttime measured and predicted peaks had a 2-h difference.

CTM simulated EC was on average driven by local domestic wood combustion (41 %), local road transport (24 %), with additional contributions from outside Barcelona (27 %), local agriculture and waste burning (3 %) and local shipping (3 %). 68 % of the transported EC was related to domestic wood combustion, 26 % to sources outside Europe, 3 % to domestic combustion from other fuels (coal, liquid, gas) and the remaining due to wildfires and non-road transportation.

4.4.1. *Evaluation including comparison with aethalometer source apportionment*

According to results from RM, fossil fuel (mostly road traffic) was the

Table 4
Daily estimated concentrations of PM_1 BBOA during the winter period.

Date	BBOA (μg m^{-3}) (for BBOA: K^+_{bb}=20)	BBOA (μg m^{-3}) (lower – upper limit)
January 6, 2019	1.8	0.45–9
January 14, 2019	2	0.5–10
January 18, 2019	2.6	0.65–13
January 22, 2019	2.8	0.7–14
January 26, 2019	1.6	0.4–8
January 30, 2019	0.4	0.1–2

dominant source of eBC during wintertime based on the analysis of the aethalometer data with an average measured concentration of 0.8 μg m^{-3} and a contribution of 73 %. The diurnal trend showed a morning peak at 09:00 LT and another one early in the evening (Fig. 7a). EC levels from this source were underpredicted by the model, by a factor of 1.5, on average, indicating that emissions from these sources probably need to be revised. Hourly metrics are provided in Table 3.

eBC from biomass burning contributed 27 % of the total eBC based on the analysis of the measurements, with an average measured concentration of 0.3 μg m^{-3}. Two peaks were observed, one in the morning and another in the afternoon (Fig. 7b). However, the CTM significantly overpredicted EC from biomass burning, estimating an average concentration of 0.53 μg m^{-3} -almost two times higher than the value derived from aethalometer measurements-RM.

The current emission inventory assumes an EC to OC ratio of 2:3 for biomass burning in winter, which likely leads to an overestimation of EC emissions from this source. Revising this ratio is necessary to align with experimental studies indicating that EC often constitutes only 5–10 % of total biomass burning emissions (Kodros et al., 2020).

5. Sensitivity tests

5.1. Transportation

HOA concentrations were underestimated during the morning and evening rush hours, with this underprediction being more pronounced in winter. This suggests a need to revise the HOA daily emission profile, particularly by increasing emissions during these peak traffic periods. The results of a sensitivity test, in which we doubled the HOA emissions, are presented in Fig. S4. During the summer, the average HOA concentration increased from 0.21 to 0.25 μg m^{-3}, whereas in winter it rose from 0.30 to 0.4 μg m^{-3}. However, the morning and nighttime peaks show no notable improvement, indicating that actual HOA emissions are likely more than twice those estimated in the current emissions inventory. This is also reflected in the average concentrations of PM_1 total and primary OA across the entire urban domain, which show no significant changes after doubling the HOA emissions (Fig. S5).

5.2. Cooking

Based on ACSM measurements, cooking was identified as a significant source of OA in the city during both summer and winter periods, contributing approximately 11 % of total PM_1 OA in each season. To assess the potential influence of underestimated cooking emissions, a sensitivity test was conducted by incorporating an additional 1140 kg d^{-1} of COA emissions for the whole modeling domain. This value is consistent with Siouti et al. (2021), who estimated that COA emissions can be up to 2.5 times higher than primary OA emissions included in the current emission inventory. The spatial distribution of COA emissions (Fig. S6) was based on the high-resolution population distribution (https://ec.europa.eu/eurostat/web/gisco/geodata/grids). As a result, model predictions for the summer period indicate that COA contributes 12 %, hydrocarbon-like OA 14 %, oxygenated OA 73 % and BBOA 1 % to the total PM_1 OA in Palau Reial in Barcelona. The average COA concentration predicted after the added emissions was equal to 0.38 μg m^{-3} and the concentration in the measurement site was 0.3 μg m^{-3}, suggesting that out estimated COA emissions are reasonable at least as a first guess. Average ground concentrations of PM_1 total and primary OA before and after the addition of COA emissions were also presented in Fig. S7, indicating the importance of this source for the urban domain.

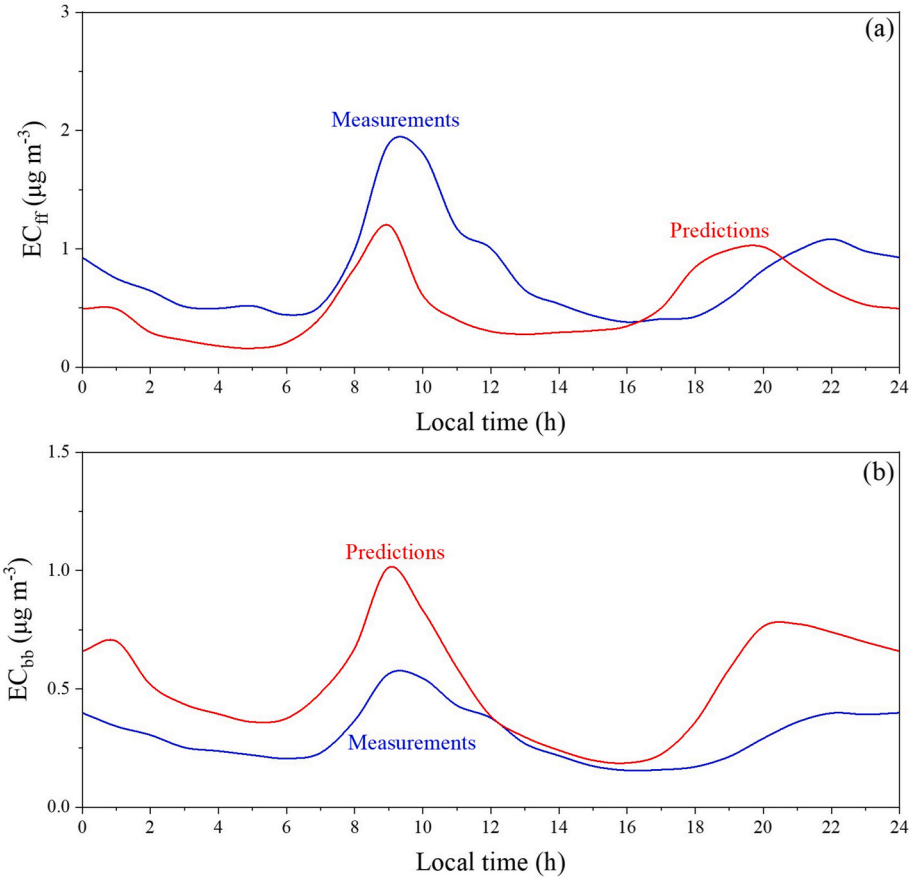

Fig. 7. Average diurnal profile of predicted EC and measured eBC from (a) fossil fuel and (b) biomass burning combustion in Palau Reial during the winter period.

6. Conclusions

During the summer, oxygenated organic aerosol was the dominant source of PM_1 OA in Barcelona. Most of this originated from sources outside the city, including wildfires, biogenic and marine sources as well as transport from regions outside Europe. The next largest contributor was COA, although this source was not included in the current emission inventory. HOA was the third most important OA component and, according to the model, was primarily attributed to transportation and to local agriculture.

During winter, OOA was surprisingly the dominant source of PM_1 OA and was seriously underestimated by the model. Based on potassium (K) measurements, aged BBOA could explain a significant fraction of the discrepancy between measurements and predictions. This indicates that regional biomass burning sources are underestimated in the used emission inventory and at the same time there are one or more important processes converting the fresh BBOA to SOA effectively during periods of low photochemical activity. Nighttime and aqueous phase chemistry are both good candidates. Fresh BBOA contributed 11 % to the total PM_1 OA, but it was underpredicted by the model, probably again due to the underestimation of this source in the emission inventory. Local transportation was the second most important source of OA during wintertime (14 %), but it was also underpredicted by the model by a factor of four during peak hours. Cooking was an important source also in winter (11 %), but it is missing from the emission inventories. Emissions of approximately 1100 kg d^{-1} of COA are needed to account for this significant missing source in the model.

The dominant source of EC was fossil fuel (mostly road traffic) combustion (73–74 % of total EC) with lower contribution from biomass burning for both periods. The existing emission inventory appears to overestimate EC from biomass burning during winter and to underestimate this source during summer, while it underestimates the transportation contribution for both periods.

Differences between modeled and measured concentrations may arise from missing or underestimated emission sources, unaccounted reaction mechanisms such as nighttime chemistry of BBOA, or the need for improved representation of secondary formation processes. In addition, inaccuracies in meteorological predictions may also contribute to these differences.

Accurate model predictions of PM concentrations and their sources, combined with high-quality measurements, are essential for understanding pollution origins in urban areas. In addition, back-trajectory analysis could be helpful to better understand the potential source areas of the pollutants transported to Barcelona. Integrating measurements with modeling enables the identification of sources, including those that are difficult to measure or not directly observed through monitoring. This comprehensive approach supports the development of effective policies to reduce emissions and improve air quality.

CRediT authorship contribution statement

Evangelia Siouti: Writing – review & editing, Writing – original draft, Software, Methodology, Investigation, Formal analysis. **Ksakousti Skyllakou:** Writing – review & editing, Methodology, Investigation. **David Patoulias:** Writing – review & editing, Investigation. **Eleni Athanasopoulou:** Writing – review & editing, Software, Investigation. **Jeroen Kuenen:** Writing – review & editing, Methodology. **Marta Via:** Writing – review & editing, Investigation, Formal analysis. **Marjan Savadkoohi:** Writing – review & editing, Investigation, Formal analysis. **María Cruz Minguillón:** Writing – review & editing, Investigation, Data curation. **Marco Pandolfi:** Writing – review & editing, Investigation. **Andrés Alastuey:** Writing – review & editing, Investigation. **Xavier Querol:** Writing – review & editing, Supervision, Methodology. **Spyros N. Pandis:** Writing – review & editing, Supervision, Methodology, Conceptualization.

Declaration of competing interest

The authors declare that they have no known competing financial interests or personal relationships that could have appeared to influence the work reported in this paper.

Acknowledgements

This work was supported by the EU H2020 Research Infrastructures Services Reinforcing Air Quality Monitoring Capacities in European Urban & Industrial AreaS (RI-URBANS) project (grant 101036245). The authors acknowledge the Aerosol d.o.o. Company for providing the AE33 instrument for the Barcelona station.

Appendix A. Supplementary data

Supplementary data to this article can be found online at https://doi.org/10.1016/j.atmosenv.2025.121761.

Data availability

Data will be made available on request.

References

Allan, J.D., Delia, A.E., Coe, H., Bower, K.N., Alfarra, M.R., Jimenez, J.L., Middlebrook, A.M., Drewnick, F., Onasch, T.B., Canagaratna, M.R., Jayne, J.T., Worsnop, D.R., 2004. A generalised method for the extraction of chemically resolved mass spectra from Aerodyne aerosol mass spectrometer data. J. Aerosol Sci. 35, 909–922. https://doi.org/10.5194/acp-6-5279-2006.

Benavides, J., Snyder, M., Guevara, M., Soret, A., Pérez García-Pando, C., Amato, F., Querol, X., Jorba, O., 2019. CALIOPE-Urban v1.0: coupling R-LINE with a mesoscale air quality modelling system for urban air quality forecasts over Barcelona city (Spain). Geosci. Model Dev. (GMD) 12, 2811–2835. https://doi.org/10.5194/gmd-12-2811-2019.

Bond, T.C., Bergstrom, R.W., 2006. Light absorption by carbonaceous particles: an investigative review. Aerosol Sci. Technol. 40, 27–67. https://doi.org/10.1080/02786820500421521.

Briggs, N.L., Long, C.M., 2016. Critical review of black carbon and elemental carbon source apportionment in Europe and the United States. Atmos. Environ. 144, 409–427.

Canonaco, F., Tobler, A., Chen, G., Sosedova, Y., Slowik, J.G., Bozzetti, C., Daellenbach, K.R., El Haddad, I., Crippa, M., Huang, R.-J., Furger, M., Baltensperger, U., Prevot, 2021. A new method for long-term source apportionment with time-dependent factor profiles and uncertainty assessment using SoFi Pro: application to 1 year of organic aerosol data. Atmos. Meas. Tech. 14, 923–943. https://doi.org/10.5194/amt-14-923-2021.

Cao, F., Zhang, S.C., Kawamura, K., Zhang, Y.L., 2016. Inorganic markers, carbonaceous components and stable carbon isotope from biomass burning aerosols in Northeast China. Sci. Total Environ. 572, 1244–1251.

Capaldo, K., Pilinis, C., Pandis, S.N., 2000. A computationally efficient hybrid approach for the simulation of dynamic gas/aerosol transfer in air quality models. Atmos. Environ. 34, 3617–3627.

Carter, W.P.L., 2000. Documentation of the SAPRC-99 chemical mechanism for VOC reactivity assessment. Report to California air resources board. Available online: https://intra.engr.ucr.edu/~carter/absts.htm#saprc99.

Cavalli, F., Viana, M., Yttri, K.E., Genberg, J., Putaud, J.-P., 2010. Toward a standardised thermal-optical protocol for measuring atmospheric organic and elemental carbon: the EUSAAR protocol. Atmos. Meas. Tech. 3, 79–89. https://doi.org/10.5194/amt-3-79-2010.

Chen, G., Canonaco, F., Tobler, A., Aas, W., Alastuey, A., Allan, J., Atabakhsh, S., Aurela, M., Baltensperger, U., Bougiatioti, A., De Brito, J.F., Ceburnis, D., Chazeau, B., Chebaicheb, H., Daellenbach, K.R., Ehn, M., El Haddad, I., Eleftheriadis, K., Favez, O., Flentje, H., Font, A., Fossum, K., Freney, E., Gini, M., Green, D.C., Heikkinen, L., Herrmann, H., Kalogridis, A.-C., Keernik, H., Lhotka, R., Lin, C., Lunder, C., Maasikmets, M., Manousakas, M.I., Marchand, N., Marin, C., Marmureanu, L., Mihalopoulos, N., Močnik, G., Nęcki, J., O'Dowd, C., Ovadnevaite, J., Peter, T., Petit, J.-E., Pikridas, M., Platt, S.M., Pokorná, P., Poulain, L., Priestman, M., Riffault, V., Rinaldi, M., Różański, K., Schwarz, J., Sciare, J., Simon, L., Skiba, A., Slowik, J.G., Sosedova, Y., Stavroulas, I., Styszko, K., Teinemaa, E., Timonen, H., Tremper, A., Vasilescu, J., Via, M., Vodička, P., Wiedensohler, A., Zografou, O., Minguillón, M.C., Prévôt, A.S.H., 2022. European aerosol phenomenology – 8: harmonised source apportionment of organic aerosol using 22 year-long ACSM/AMS datasets. Environ. Int. 166, 107325.

COST COLOSSAL, 2019. COST Action CA16109 COLOSSAL Chemical On-Line cOmposition and Source Apportionment of fine aerosoL, Working Group 1, Guidelines for comparison of ACSM measurement with co-located external data.

Deliverable 1.2. Released in December 2019. http://www.actris-ecac.eu/pmc-non-refractory-organics-and-inorganics.html.
DeCarlo, P.F., Dunlea, E.J., Kimmel, J.R., Aiken, A.C., Sueper, D., Crounse, J., Wennberg, P.O., Emmons, L., Shinozuka, Y., Clarke, A., Zhou, J., Tomlinson, J., Collins, D.R., Knapp, D., Weinheimer, A.J., Montzka, D.D., Campos, T., Jimenez, J.L., 2008. Fast airborne aerosol size and chemistry measurements above Mexico City and Central Mexico during the MILAGRO campaign. Atmos. Chem. Phys. 8, 4027–4048. https://doi.org/10.5194/acp-8-4027-2008.
Donahue, N.M., Robinson, A.L., Stanier, C.O., Pandis, S.N., 2006. Coupled partitioning, dilution, and chemical aging of semivolatile organics. Environ. Sci. Technol. 40, 2635–2643.
Drewnick, F., Hings, S., De Carlo, P., Jayne, J., Gonin, M., Fuhrer, K., Weimer, S., Jimenez, J., Demerjian, K., Borrmann, S., Worsnop, D., 2005. A new time-of-flight aerosol mass spectrometer (TOF-AMS) – instrument description and first field deployment. Aerosol Sci. Technol. 39, 637–658. https://doi.org/10.1080/02786820500182040.
Drinovec, L., Močnik, G., Zotter, P., Prévôt, A.S.H., Ruckstuhl, C., Coz, E., Rupakheti, M., Sciare, J., Müller, T., Wiedensohler, A., Hansen, A.D.A., 2015. The "dual-spot" aethalometer: an improved measurement of aerosol black carbon with real-time loading compensation. Atmos. Meas. Tech. 8, 1965–1979. https://doi.org/10.5194/amt-8-1965-2015.
Fahey, K.M., Pandis, S.N., 2001. Optimizing model performance: variable size resolution in cloud chemistry modeling. Atmos. Environ. 35, 4471–4478.
Falkovich, A.H., Schkolnik, G., 2004. Adsorption of organic compounds pertinent to urban environments onto mineral dust particles. J. Geophys. Res. 109, D02208.
Fountoukis, C., Racherla, P.N., Denier van der Gon, H.A.C., Polymeneas, P., Charalambidis, P.E., Pilinis, C., Wiedensohler, A., Dall'Osto, M., O'Dowd, C., Pandis, S.N., 2011. Evaluation of a three-dimensional chemical transport model (PMCAMx) in the European domain during the EUCAARI May 2008 campaign. Atmos. Chem. Phys. 11, 10331–10347.
Fourtziou, L., et al., 2017. Multi-tracer approach to characterize domestic wood burning in Athens (Greece) during wintertime. Atmos. Environ. 148, 89–101.
Gaydos, T.M., Koo, B., Pandis, S.N., Chock, D.P., 2003. Development and application of an efficient moving sectional approach for the solution of the atmospheric aerosol condensation/evaporation equation. Atmos. Environ. 37, 3303–3316.
Guenther, A.B., Jiang, X., Heald, C.L., Sakulyanontvittaya, T., Duhl, T., Emmons, L.K., Wang, X., 2012. The Model of Emissions of Gases and Aerosols from Nature version 2.1 (MEGAN2.1): an extended and updated framework for modeling biogenic emissions. Geosci. Model Dev. 5, 1471–1492. https://doi.org/10.5194/gmd-5-1471-2012.
Ho, K.F., Lee, S.C., Chow, J.C., Watson, J.G., 2003. Characterization of PM_{10} and $PM_{2.5}$ source profiles for fugitive dust in Hong Kong. Atmos. Environ. 37, 1023–1032.
IPCC, 2021. In: Masson-Delmotte, V., Zhai, P., Pirani, A., Connors, S.L., Péan, C., Berger, S., Caud, N., Chen, Y., Goldfarb, L., Gomis, M.I., Huang, M., Leitzell, K., Lonnoy, E., Matthews, J.B.R., Maycock, T.K., Waterfield, T., Yelekçi, O., Yu, R., Zhou, B. (Eds.), Climate Change 2021: the Physical Science Basis. Contribution of Working Group I to the Sixth Assessment Report of the Intergovernmental Panel on Climate Change. Cambridge University Press.
Jayne, J.T., Leard, D.C., Zhang, X., Davidovits, P., Smith, K.A., Kolb, C.E., Worsnop, D.R., 2000. Development of an aerosol mass spectrometer for size and composition analysis of submicron particles. Aerosol Sci. Technol. 33, 49–70.
Jimenez, J., Canagaratna, M., Donahue, N., Prevot, A., Zhang, Q., Kroll, J., DeCarlo, P., Allan, J., Coe, H., Ng, N., Aiken, A., Docherty, K., Ulbrich, I., Grieshop, A., Robinson, A., Duplissy, J., Smith, J., Wilson, K., Lanz, V., Hueglin, C., Sun, Y., Tian, J., Laaksonen, A., Raatikainen, T., Rautiainen, J., Vaattovaara, P., Ehn, M., Kulmala, M., Tomlinson, J., Collins, D., Cubison, M., Dunlea, E., Huffman, J., Onasch, T., Alfarra, M., Williams, P., Bower, K., Kondo, Y., Schneider, J., Drewnick, F., Borrmann, S., Weimer, S., Demerjian, K., Salcedo, D., Cottrell, L., Griffin, R., Takami, A., Miyoshi, T., Hatakeyama, S., Shimono, A., Sun, J., Zhang, Y., Dzepina, K., Kimmel, J., Sueper, D., Jayne, J., Herndon, S., Trimborn, A., Williams, L., Wood, E., Middlebrook, A., Kolb, C., Baltensperger, U., Worsnop, D., 2009. Evolution of organic aerosols in the atmosphere. Science 326, 1525–1529. https://doi.org/10.1126/science.1180353.
Kchik, H., Perrino, C., Cherif, S., 2015. Investigation of desert dust contribution to source apportionment of PM_{10} and $PM_{2.5}$ from a southern Mediterranean coast. Aerosol Air Qual. Res. 15, 454–464.
Kiendler-Scharr, A., Mensah, A.A., Friese, E., Topping, D., Nemitz, E., Prevot, A.S.H., Äijälä, M., Allan, J., Canonaco, F., Canagaratna, M., Carbone, S., Crippa, M., Dall'Osto, M., Day, D.A., De Carlo, P., Di Marco, C.F., Elbern, H., Eriksson, A., Freney, E., Hao, L., Herrmann, H., Hildebrandt, L., Hillamo, R., Jimenez, J.L., Laaksonen, A., McFiggans, G., Mohr, C., O'Dowd, C., Otjes, R., Ovadnevaite, J., Pandis, S.N., Poulain, L., Schlag, P., Sellegri, K., Swietlicki, E., Tiitta, P., Vermeulen, A., Wahner, A., Worsnop, D., Wu, H.C., 2016. Ubiquity of organic nitrates from nighttime chemistry in the European submicron aerosol. Geophys. Res. Lett. 43, 7735–7744. https://doi.org/10.1002/2016GL069239.
Kodros, J.K., Kaltsonoudis, C., Paglione, M., Florou, K., Jorga, S., Vasilakopoulou, C., Cirtog, M., Cazaunau, M., Picquet-Varrault, B., Nenes, A., Pandis, S.N., 2022. Secondary aerosol formation during the dark oxidation of residential biomass burning emissions. Environ. Sci. Atmos 2, 1221–1236. https://doi.org/10.1039/d2ea00031h.
Kodros, J.K., Papanastasiou, D.K., Paglione, M., Masiol, M., Squizzato, S., Florou, K., Skyllakou, K., Kaltsonoudis, C., Nenes, A., Pandis, S.N., 2020. Rapid dark aging of biomass burning as an overlooked source of oxidized organic aerosol. Proc. Natl. Acad. Sci. USA 117, 33028–33033. https://doi.org/10.1073/pnas.2010365117.
Koo, B.Y., Wilson, G.M., Morris, R.E., Dunker, A.M., Yarwood, G., 2009. Comparison of source apportionment and sensitivity analysis in a particulate matter air quality model. Environ. Sci. Technol. 43, 6669–6675.
Kuenen, J., Dellaert, S., Visschedijk, A., Jalkanen, J.P., Denier van der Gon, H., 2022. CAMS-REG-v4: a state-of-the-art high-resolution European emission inventory for air quality modelling. Earth Syst. Sci. Data 14, 491–515.
Kumar, A., Goel, V., Faisal, M., Ali, U., Maity, R., Ganguly, D., Singh, V., Kumar, M., 2024. Two different approaches for source apportionment of ambient black carbon in highly polluted environments. Atmos. Environ. 338, 120863.
Lai, S.C., Zou, S.C., Cao, J.J., Lee, S.C., Ho, K.F., 2007. Characterizing ionic species in $PM_{2.5}$ and PM_{10} in four Pearl River Delta cities, South China. Environ. Sci. 19, 939–947.
Liu, H., Wang, Q., Xing, L., Zhang, Y., Zhang, T., Ran, W., Cao, J., 2021. Measurement report: quantifying source contribution of fossil fuels and biomass-burning black carbon aerosol in the southeastern margin of the Tibetan Plateau. Atmos. Chem. Phys. 21, 973–987.
Liu, Y., Yan, C., Zheng, M., 2018. Source apportionment of black carbon during winter in Beijing. Sci. Total Environ. 618, 531–541.
Middlebrook, A.M., Bahreini, R., Jimenez, J.L., Canagaratna, M.R., 2012. Evaluation of composition-dependent collection efficiencies for the Aerodyne aerosol mass spectrometer using field data. Aerosol Sci. Technol. 46, 258–271. https://doi.org/10.1080/02786826.2011.620041.
Minguillón, M.C., Pérez, N., Marchand, N., Bertrand, A., Temime-Roussel, B., Agrios, K., Szidat, S., van Drooge, B., Sylvestre, A., Alastuey, A., Reche, C., Ripoll, A., Marco, E., Grimalt, J.O., Querol, X., 2016. Secondary organic aerosol origin in an urban environment: influence of biogenic and fuel combustion precursors. Faraday Discuss 189, 337–359.
Mohr, C., DeCarlo, P.F., Heringa, M.F., Chirico, R., Slowik, J.G., Richter, R., Reche, C., Alastuey, A., Querol, X., Seco, R., Peñuelas, J., Jiménez, J.L., Crippa, M., Zimmermann, R., Baltensperger, U., Prévôt, A.S.H., 2012. Identification and quantification of organic aerosol from cooking and other sources in Barcelona using aerosol mass spectrometer data. Atmos. Chem. Phys. 12, 1649–1665.
Monahan, E.C., Spiel, D.E., Davidson, K.L. (1986). A model of marine aerosol generation via whitecaps and wave disruption. In *Oceanic Whitecaps*, Monahan, E.C., Niocaill, G. M., Eds., Springer: Dordrecht, The Netherlands, 1986, Volume 2, pp. 167–174.
Morris, R.E., McNally, D.E., Tesche, T.W., Tonnesen, G., Boylan, J.W., Brewer, P., 2005. Preliminary evaluation of the Community Multiscale Air Quality model for 2002 over the southeastern United States. J. Air Waste Manag. Assoc. 55, 1694–1708.
Ng, N.L., Canagaratna, M.R., Zhang, Q., Jimenez, J.L., Tian, J., Ulbrich, I.M., Kroll, J.H., Docherty, K.S., Chhabra, P.S., Bahreini, R., Murphy, S.M., Seinfeld, J.H., Hildebrandt Ruiz, L., Yatavelli, R.L.N., Sueper, D., Dunlea, E., Smith, K.A., Worsnop, D.R., 2011. An aerosol chemical speciation monitor (ACSM) for routine monitoring of the composition and mass concentrations of ambient aerosol. Aerosol. Sci. Technol. 45, 780–794. https://doi.org/10.1080/02786826.2011.560211.
O'Dowd, C.D., Langmann, B., Varghese, S., Scannell, C., Ceburnis, D., Facchini, M.C., 2008. A combined organic-inorganic sea-spray source function. Geophysical Research Letters 35, L01801. https://doi.org/10.1029/2007GL030331.
Paatero, P., 1999. The Multilinear Engine – a table-driven, least squares program for solving multilinear problems, including the n-way parallel factor analysis model. J. Comput. Graph Stat. 8, 854–888.
Park, R.J., Jacob, D.J., Chin, M., Martin, R.V., 2003. Sources of carbonaceous aerosols over the United States and implications for natural visibility. J. Geophys. Res. 108, 4355. https://doi.org/10.1029/2002JD003190.
Petit, J.-E., Favez, O., Sciare, J., Canonaco, F., Croteau, P., Močnik, G., Jayne, J., Worsnop, D., Leoz-Garziandia, E., 2014. Submicron aerosol source apportionment of wintertime pollution in Paris, France by double positive matrix factorization (PMF^2) using an aerosol chemical speciation monitor (ACSM) and a multi-wavelength aethalometer. Atmos. Chem. Phys. 14, 13773–13787. https://doi.org/10.5194/acp-14-13773-2014.
Petzold, A., Ogren, J.A., Fiebig, M., Laj, P., Li, S.-M., Baltensperger, U., Holzer-Popp, T., Kinne, S., Pappalardo, G., Sugimoto, N., Wehrli, C., Wiedensohler, A., Zhang, X.-Y., 2013. Recommendations for reporting "black carbon" measurements. Atmos. Chem. Phys. 13, 8365–8379.
Querol, X., Alastuey, A., Rodriguez, S., Plana, F., Ruiz, C.R., Cots, N., Massagué, G., Puig, O., 2001. PM_{10} and $PM_{2.5}$ source apportionment in the Barcelona Metropolitan area, Catalonia, Spain. Atmos. Environ. 35 (36), 6407–6419.
Ramacher, M.O.P., Kakouri, A., Speyer, O., Feldner, J., Karl, M., Timmermans, R., Denier van der Gon, H., Kuenen, J., Gerasopoulos, E., Athanasopoulou, E., 2021. The UrbEm hybrid method to derive high-resolution emissions for city-scale air quality modeling. Atmosphere 12, 1404. https://doi.org/10.3390/atmos12111404.
Sandradewi, J.A., Prévôt, A.S.H., Szidat, S., Perron, N., Alfarra, M.R., Lanz, V.A., Weingartner, E., Baltensperger, U., 2008. Using aerosol light absorption measurements for the quantitative determination of wood burning and traffic emission contributions to particulate matter. Environ. Sci. Technol. 42, 3316–3323.
Savadkoohi, M., Pandolfi, M., Favez, O., Putaud, J.-P., Eleftheriadis, K., Fiebig, M., Hopke, P.K., Laj, P., Wiedensohler, A., Alados-Arboledas, L., Bastian, S., Chazeau, B., María, A.C., Colombi, C., Costabile, F., Green, D.C., Hueglin, C., Liakakou, E., Luoma, K., Listrani, S., Mihalopoulos, E., Marchand, E., Močnik, G., Niemi, J.V., Ondráček, J., Petit, J.-E., Rattigan, O.V., Reche, C., Timonen, H., Titos, G., Tremper, A.H., Vratolis, S., Vodička, P., Funes, E.Y., Zíková, N., Harrison, R.M., Petäjä, T., Alastuey, A., Querol, X., 2024. Recommendations for reporting equivalent black carbon (eBC) mass concentrations based on long-term Pan-European in-situ observations. Environ. Int. 185, 108553. https://doi.org/10.1016/j.envint.2024.108553.
Savadkoohi, M., Pandolfi, M., Reche, C., Niemi, J.V., Mooibroek, D., Titos, G., Green, D. C., Tremper, A.H., Hueglin, C., Coz, E., Liakakou, E., Mihalopoulos, N., Stavroulas, I.,

Alados-Arboledas, L., Beddows, D., Brito, J.F.D., Bastian, S., Baudic, A., Colombi, C., Costabile, F., Estell, V., Matos, V., Gaag, E.V., Silvergren, S., Petit, J., Putaud, J., Rattigan, O.V., Timonen, H., Tuch, T., Merkel, M., Weinhold, K., Vratolis, S., Vasilescu, J., Favez, O., Harrison, R.M., Laj, P., Wiedensohler, A., Hopke, P.K., Pet, T., Querol, X., 2023. The variability of mass concentrations and source apportionment analysis of equivalent black carbon across urban Europe. Environ. Int. J 178. https://doi.org/10.1016/j.envint.2023.108081.

Seinfeld, J.H., Pandis, S.N., 2016. Atmospheric Chemistry and Physics: from Air Pollution to Climate Change. John Wiley & Sons.

Siouti, E., Skyllakou, K., Kioutsioukis, I., Ciarelli, G., Pandis, S.N., 2021. Simulation of the cooking organic aerosol concentration variability in an urban area. Atmospheric Environment 265, 118710.

Siouti, E., Skyllakou, K., Kioutsioukis, I., Patoulias, D., Apostolopoulos, I.D., Fouskas, G., Pandis, S.N., 2024. Prediction of the concentration and source contributions of $PM_{2.5}$ and gas-phase pollutants in an urban area with the SmartAQ forecasting system. Atmosphere 15, 8.

Siouti, E., Skyllakou, K., Kioutsioukis, I., Patoulias, D., Fouskas, G., Pandis, S.N., 2022. Development and application of the SmartAQ high-resolution air quality and source apportionment forecasting system for European urban areas. Atmosphere 13, 1693. https://doi.org/10.3390/atmos13101693.

Siouti, E., Skyllakou, K., Patoulias, D., Athanasopoulou, E., Mihalopoulos, N., Kuenen, J., Pandis, S.N., 2025. High resolution source-resolved $PM_{2.5}$ spatial distribution and human exposure in a large urban area. Atmos. Environ., 121277 https://doi.org/10.1016/j.atmosenv.2025.121277.

Skamarock, W.C., Klemp, J.B., Dudhia, J., Gill, D.O., Liu, Z., Berner, J., Wang, W., Powers, J.G., Duda, M.G., Barker, D.M., 2019. A description of the advanced research WRF model version 4.1. https://doi.org/10.5065/1dfh-6p97(No.NCAR/TN-556+STR.

Skyllakou, K., Fountoukis, C., Charalampidis, P., Pandis, S.N., 2017. Volatility-resolved source apportionment of primary and secondary organic aerosol over Europe. Atmos. Environ. 167, 1–10.

Slinn, S.A., Slinn, W.G.N., 1980. Predictions for particle deposition on natural waters. Atmos. Environ. 14, 1013–1016. https://doi.org/10.1016/0004-6981(80)90032-3.

Soret, A., Guevara, M., Baldasano, J.M., 2014. The potential impacts of electric vehicles on air quality in the urban areas of Barcelona and Madrid (Spain). Atmos. Environ. 99, 51–63.

Tambour, Y., Seinfeld, J.H., 1980. Solution of the discrete coagulation equation. J. Colloid Interface Sci. 74, 260–272.

Tiitta, P., Leskinen, A., Hao, L., Yli-Pirilä, P., Kortelainen, M., Grigonyte, J., Tissari, J., Lamberg, H., Hartikainen, A., Kuuspalo, K., Kortelainen, A.-M., Virtanen, A., Lehtinen, K.E.J., Komppula, M., Pieber, S., Prévôt, A.S.H., Onasch, T.B., Worsnop, D. R., Czech, H., Zimmermann, R., Jokiniemi, J., Sippula, O., 2016. Transformation of logwood combustion emissions in a smog chamber: formation of secondary organic aerosol and changes in the primary organic aerosol upon daytime and nighttime aging. Atmos. Chem. Phys. 16, 13251–13269. https://doi.org/10.5194/acp-16-13251-2016.

Tsimpidi, A.P., Karydis, V.A., Zavala, M., Molina, L., Ulbrich, I., Jimenez, J.L., Pandis, S. N., 2010. Evaluation of the volatility basis-set approach for the simulation of organic aerosol formation in the Mexico City metropolitan area. Atmos. Chem. Phys. 10, 525–546.

Via, M., Minguillón, M.C., Reche, C., Querol, X., Alastuey, A., 2021. Increase in secondary organic aerosol in an urban environment. Atmos. Chem. Phys. 21, 8323–8339. https://doi.org/10.5194/acp-21-8323-2021.

Wagstrom, K.M., Pandis, S.N., Yarwood, G., Wilson, G.M., Morris, R.E., 2008. Development and application of a computationally efficient particulate matter apportionment algorithm in a three-dimensional chemical transport model. Atmos. Environ. 42, 5650–5659.

Wang, Y., Zhuang, G., Sun, Y., An, Z., 2006. The variation of characteristics and formation mechanisms of aerosols in dust, haze and clear days in Beijing. Atmos. Environ. 40, 6579–6591.

Wesely, M.L., 2007. Parameterization of surface resistances to gaseous dry deposition in regional-scale numerical models. Atmos. Environ. 41, 52–63. https://doi.org/10.1016/j.atmosenv.2007.10.058.

WHO, 2024. Ambient (Outdoor) Air Pollution. World Health Organization. https://www.who.int/news-room/fact-sheets/detail/ambient-(outdoor)-air-quality-and-health.

Zhang, R., Shen, Z., Cheng, T., Zhang, M., Liu, Y., 2010. The elemental composition of atmospheric particles at Beijing during Asian dust events in Spring 2004. Aerosol Air Qual. Res. 10, 67–75.

Zografou, O., Gini, M., Manousakas, M.I., Chen, G., Kalogridis, A.C., Diapouli, E., Pappa, A., Eleftheriadis, K., 2022. Combined organic and inorganic source apportionment on yearlong ToF-ACSM dataset at a suburban station in Athens. Atmos. Meas. Tech. 15, 4675–4692. https://doi.org/10.5194/amt-15-4675-2022.

Zotter, P., Ciobanu, V.G., Zhang, Y.L., El-Haddad, I., Macchia, M., Daellenbach, K.R., Salazar, G.A., Huang, R.-J., Wacker, L., Hueglin, C., Piazzalunga, A., Fermo, P., Schwikowski, M., Baltensperger, U., Szidat, S., Prévôt, A.S.H., 2014. Radiocarbon analysis of elemental and organic carbon in Switzerland during winter-smog episodes from 2008 to 2012 – part 1: source apportionment and spatial variability. Atmos. Chem. Phys. 14, 13551–13570.